Synthesis and Light Scattering Study of Hydroxypropyl Cellulose Microgels

Xihua Lu, Zhibing Hu,* and Jun Gao

Departments of Physics and Materials Science, University of North Texas, Denton, Texas 76203

Received May 4, 2000; Revised Manuscript Received September 7, 2000

ABSTRACT: The thermally responsive hydroxypropyl cellulose (HPC) microgels have been synthesized and characterized. The microgel particles were obtained by chemically cross-linking collapsed HPC polymer chains in water−surfactant (dodecyltrimethylammonium bromide) dispersion above the lower critical solution temperature of the HPC. The size distributions of microgel particles, measured by dynamic light scattering, have been correlated with synthesis conditions including surfactant concentration, polymer concentration, and reaction temperature. The final microgel size is determined by the balance between the hydrophobic interaction among HPC polymer chains and intermicelle electrostatic repulsion. The swelling and phase transition properties of resultant HPC microgels have been analyzed using both static and dynamic light scattering techniques as a function of temperature and cross-linker concentration. It is found that the increase in the cross-linker concentration reduces the shrinkage extent. The dilute HPC microgel particles ($C < 1.0 \times 10^{-5}$ g/mL) form a stable colloidal dispersion at room temperature and at 44 °C (above the volume phase transition temperature), probably due to steric effects. Adding salt to water leads to a decrease of the volume phase transition temperature of HPC microgels.

Introduction

Microgels are cross-linked colloidal particles that can swell by the absorption of many times their weight of solvent and exhibit a behavior ranging from that of polymer solutions to that of hard spheres.[1−4] Regarding a dispersion of identical colloidal particles as a one-component assembly of superatoms dispersed in a continuous background, microgel systems lead the fundamental study of modeling the transition from liquid to crystal and from the supercooled liquid to the glassy state of atomic fluids.[4] From an application point of view, the microgel particles can respond to the environmental change much faster than bulk gels due to much smaller size of the particles.[5] Unusual properties of microgels lead to various applications including the automotive surface coatings,[6] the printing,[7] and controlled drug delivery.[8,9]

Many methods have been developed for preparing micorgels, including emulsion polymerization,[10] inverse microemulsion polymerization,[11] anionic copolymerization,[12] and cross-linking of neighboring polymer chains.[13] Currently, thermally responsive microgels as represented by *N*-isopropylacrylamide (NIPA) have attracted great attention due to their scientific importance and technological applications.[1] The NIPA microgel was first synthesized by Pelton and Chibante in 1986.[10] In their study, the pre-gel solution of the NIPA monomer was heated above the lower critical solution temperature (LCST) of the NIPA polymer solution. The polymerization of the NIPA monomers and cross-linking polymer chains occurred simultaneously at the reaction temperatures above the LCST. Narrowly distributed NIPA microgel particles were obtained with their swelling properties similar to those of the bulk NIPA gel.[14]

In this paper, we report synthesis and study of another important thermally responsive microgel—hydroxypropyl cellulose (HPC). Bulk HPC hydrogel including homogeneous gel and porous gel have been extensively studied before.[15,16] The HPC gel collapses and shrinks above the volume phase transition temperature T_c around 43 °C but swells and expands below T_c. In contrast to most synthetic gels that are made from carcinogenic or teratogenic monomers, the HPC gels comprise natural cellulose ether macromolecules approved by the United States Food and Drug Administration (FDA) and thus have significant practical advantages over the synthetic gels.[16] The chemical structure of the HPC is shown in Figure 1.[17]

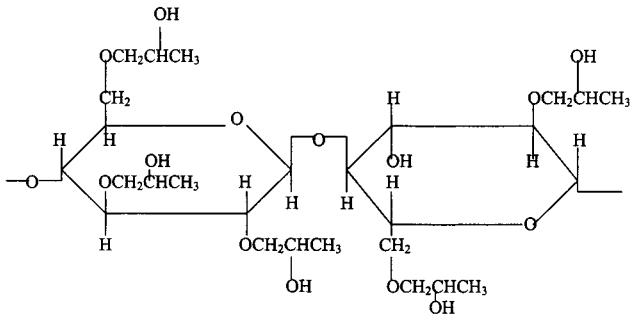

Figure 1. Chemical structure of the HPC polymer.

To our knowledge, however, synthesis of the HPC microgels has not been reported. In contrast to previous work on the NIPA microgel that started from NIPA monomers, we demonstrated the process whereby HPC chains in a surfactant solution were heated above the LCST to give colloidal particles that were then cross-linked to form microgel particles. In this paper, our results will be divided into two parts. The first is to discuss synthesis of HPC microgels that involved fundamental interaction between high molecular weight polymer chains and surfactant. The second is to discuss swelling properties and the volume phase transition of HPC microgel particles as a function of temperature, cross-linker concentration, and quality of solvent. Light scattering techniques have been used for both monitoring microgel formation and characterizing the microgel particles. Such techniques have been widely used to study various microgels.[18,19]

* To whom the correspondence should be addressed.

10.1021/ma000776k CCC: $19.00
Published on Web 10/21/2000

Table 1. Synthesis Conditions,[a] Average Radii $\langle R_h \rangle$, and Polydispersity Index ($\mu_2/\bar{\Gamma}^2$) of HPC Microgels

0.1 wt % HPC (mL)	DTAB (cmc*)	DVS (g)	reaction T (LCST) (°C)	reaction time (h)	colloidally stable	$\langle R_h \rangle$ (nm)	$\mu_2/\bar{\Gamma}^2$
100	1.0	0.04	55	1	yes	182	0.308
100	1.2	0.04	61	1	yes	179	0.204
100	1.5	0.04	64	1	yes	178	0.178

[a] The reaction occurred at the lower critical solution temperature (LCST) of 0.1 wt % HPC solution at various surfactant DTAB concentrations. cmc* is the critical micelle concentration, 1.54×10^{-2} mol/L, of surfactant DTAB in pure water at 25 °C.

Experimental Section

Materials. Dry hydroxypropyl cellulose (HPC) powder (average $M_w = 1 \times 10^6$), dodecyltrimethylammonium bromide (DTAB), divinyl sulfone (DVS), sodium hydroxide (NaOH) pellets, and sodium chloride (NaCl) were purchased from Aldrich Chemical Co. The substitution level of the HPC polymer for this study was MS = 3.9, where MS is the average number of molecules of propylene oxide combined per anhydroglucose unit. Deionized and distilled water was used throughout.

HPC Microgel Synthesis. HPC hydrogel nanoparticles were synthesized using an emulsion method. A 0.1 wt % HPC aqueous solution was prepared as follows: 0.1 g of HPC powder was dispersed in 99.9 g of aqueous sodium hydroxide solution (pH = 12) by gentle stirring for a period of 4−6 days until HPC powder was thoroughly hydrolyzed. A 0.475 g sample of dodecyltrimethylammonium bromide (DTAB) was added to 100 g of 0.1 wt % HPC solution, and the solution was stirred for 60 min. Then 0.04 g of cross-linker divinyl sulfone (DVS) was added to the HPC solution. After mixing completely, the 0.1 wt % HPC solution was heated to about 55 °C. Then the color of the HPC solution changed from clear to light blue, indicating the formation of nanoparticles. The reaction lasted for 1 h at about 55 °C. The resultant microgels were dialysized four times or more to remove the surfactant and NaOH. The same procedure was used to prepare the microgels in 0.15, 0.2, 0.3, 0.4, and 0.5 wt % HPC solutions at different surfactant concentrations and at different reaction temperatures. The cross-linking mechanism is given as follows:[20]

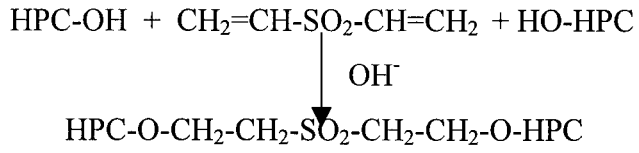

Static and Dynamic Light Scattering Characterization. A commercial laser light scattering (LLS) spectrometer (ALV/DLS/SLS-5000) equipped with an ALV-5000 digital time correlator was used with a helium−neon laser (Uniphase 1145P, output power of 22 mW and wavelength of 632.8 nm) as the light source. The incident light was vertically polarized with respect to the scattering plane, and the light intensity was regulated with a beam attenuator (Newport M-925B). The scattered light was conducted through a very thin (~ 40 μm in diameter) optical fiber leading to an active quenched avalanche photodiode (APD), the detector. As a result, the coherent factor β in dynamic laser light scattering was about 0.98. The avalanche photodiode had a sensitivity 2 orders higher than that of a normal photon multiplier (PM) tube, while its dark count increased no more than 10 times. Thus, a 22 mW laser could have a measured count rate similar to a 400 mW laser for a normal PM tube.

In static LLS, the angular dependence of the excess absolute time-averaged scattered intensity, known as the excess Rayleigh ratio $R_{vv}(q)$, was measured. For a dilute solution with a concentration C (g/mL), $R_{vv}(q)$ measured at a relatively small scattering angle θ can be written as[21]

$$\frac{KC}{R_{vv}(q)} \cong \frac{1}{M_w}\left(1 + \frac{1}{3}\langle R_g^2 \rangle_z q^2\right) + 2A_2C \qquad (1)$$

where $K = 4\pi n^2(dn/dC)^2/(N_A\lambda_0^4)$ and $q = (4\pi n/\lambda_0)\sin(\theta/2)$ with N_A, dn/dc, n, and λ_0 being Avogadro's number, the specific refractive index increment, the solvent refractive index, and the wavelength of light in a vacuum, respectively; M_w is the weight-average molar mass, A_2 is the second-order virial coefficient, and $\langle R_g^2 \rangle_z^{1/2}$ is the root-mean-square z-average radius of gyration.

In dynamic LLS, the intensity−intensity−time correlation function $G^{(2)}(t,q)$ in the self-beating mode was measured and can be expressed by[21]

$$G^{(2)}(t,q) = \langle I(t,q)\, I(q,0)\rangle = A(1 + \beta|g^{(1)}(q,t)|^2) \qquad (2)$$

where t is the decay time, A is a measured baseline, β is the coherence factor, and $g^{(1)}(q,t)$ is the normalized first-order electric field time correlation function $E(t,q)$ and is related to the line-width distribution $G(\Gamma)$ by

$$g^{(1)}(t,q) = \langle E(t,q)\, E^*(0,q)\rangle = \int_0^\infty G(\Gamma)e^{-\Gamma t}\, d\Gamma \qquad (3)$$

$G(\Gamma)$ can be obtained from the Laplace inversion of $g^{(1)}(q,t)$. $g^{(1)}(q,t)$ was analyzed by a cumulant analysis to get the average line width $\langle\Gamma\rangle$ and the relative distribution width $\mu_2/\langle\Gamma\rangle^2$. The extrapolation of Γ/q^2 to $q \to 0$ led to the translational diffusion coefficient (D). Further, $G(\Gamma)$ can be converted to the translational difffusion coefficient distribution $G(D)$ and to the hydrodynamic radius distribution $f(R_h)$ by using the Stokes−Einstein equation

$$R_h = \frac{k_B T}{6\pi\eta D} \qquad (4)$$

where k_B, T, and η are the Boltzmann constant, the absolute temperature, and the solvent viscosity, respectively. The dynamic light scattering experiments were performed at the scattering angle θ = 90°. We have carried out a typical measurement on HPC nanoparticles with their radii about 320 nm in water at room temperature and found that when the scattering angle was changed from 90° to 20°, measured particle size increased about 20% and the size distribution became narrower. Using a smaller scattering angle (<90°) could make the measurements more accurate, but it will not significantly affect the trends of the results.

Results and Discussion

A. Synthesis of HPC Microgels. The LCST of 0.1 wt % HPC increases with surfactant concentration as shown in Table 1. It is known that the pure HPC is more soluble in water at the temperatures below LCST (~41 °C) than it is at the temperatures above the LCST. This phase transition phenomenon may be explained by assuming that there are a number of equilibrium bond configurations for the propylene oxide moiety.[22−24] Each propylene oxide moiety in HPC comprises two C−O bonds and two C−C bonds. At low temperatures in polar solvents, oxygen atoms preferentially maintain a gauche orientation about C−C bonds and a trans configuration about C−O bonds.[22−24] This particular bond conformation has a relatively large dipole moment. If the temperature is increased or the solvating environment becomes less polar, then bond conformations that have

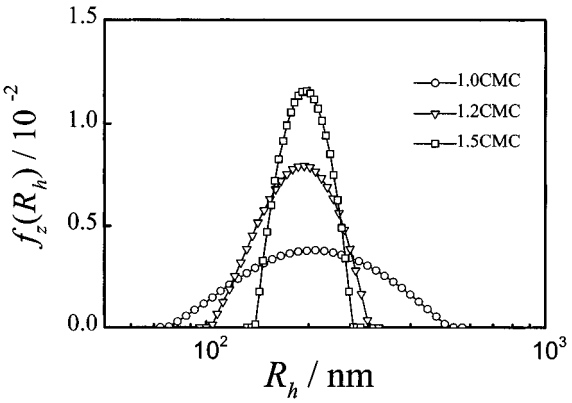

Figure 2. Hydrodynamic radius distributions ($f(R_h)$) of HPC microgel particles ($C = 8.94 \times 10^{-6}$ g/mL) in deionized water at 25 °C. These particles were prepared in 0.1 wt % HPC solution at various DTAB concentrations. Here the cmc is the critical micelle concentration of DTAB in pure water at 25 °C and equals 1.54×10^{-2} mol/L.

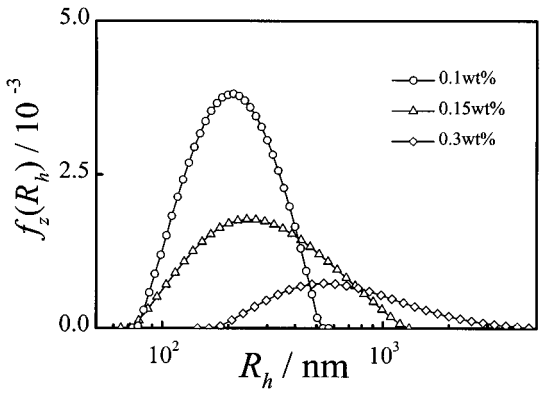

Figure 3. Hydrodynamic radius distributions ($f(R_h)$) of HPC microgel particles ($C = 8.94 \times 10^{-6}$ g/mL) in deionized water at 25 °C. These particles were prepared with various HPC concentrations at 1 cmc DTAB and at the reaction temperature 55 °C.

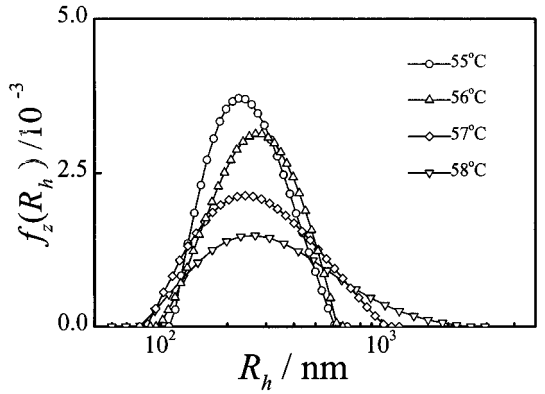

Figure 4. Hydrodynamic radius distributions ($f(R_h)$) of HPC microgel particles ($C = 8.94 \times 10^{-6}$ g/mL) in deionized water at 25 °C. These particles were made at various reaction temperatures in 0.1 wt % HPC solution and at 1 cmc DTAB concentration.

a less dipolar moment may become more favorable. The dipole moment of the propylene oxide moieties may be reduced to such an extent that phase separation occurs.[22−24]

After introducing cationic surfactant DTAB into nonionic HPC polymer in water, surfactant molecules self-assemble on the polymer chains, forming aggregates when a critical aggregation concentration is reached.[25] These aggregates are smaller in size than micelles. As more surfactant molecules accumulate on the HPC linear polymer, the micelles formed eventually. When the surfactant concentration exceeds the cmc, which is the critical micelle concentration (1.54×10^{-2} mol/L) of DTAB in pure water at 25 °C,[26] the number of absorbed surfactant aggregates increases. The polymer chains attached with surfactant micelles become more hydrophilic due to the interaggregate electrostatic repulsion. As a result, the LCST of the HPC dispersion increases with surfactant concentration.

It is found that HPC polymer chains in water−surfactant solution can collapse into colloidal particles at the LCST for DTAB surfactant concentrations ranging from 1 cmc to 1.5 cmc. Below 1 cmc, only very large particles (~10 μm) were observed. The collapsed polymer chains were stabilized by the charges on surfactant micelles that are attached on the polymer chains. Then collapsed HPC polymer chains in each colloid were chemically cross-linked by divinyl sulfone and formed microgel particles. Figure 2 shows hydrodynamic radius distributions ($f(R_h)$) of HPC microgels ($C = 8.94 \times 10^{-6}$ g/mL) in deionized water at 25 °C. These particles were prepared in 0.1 wt % HPC solution with various DTAB concentrations at the LCST that corresponds to each DTAB concentration. In the surfactant concentration range studied, the average radii $\langle R_h \rangle$ of the microgels were about the same. However, the radius distribution $f(R_h)$ becomes narrower with the increase of the surfactant concentration. This phenomenon could be due to the formation of more micelles in higher surfactant concentrations. The more charged micelles, the stronger the electrostatic repulsion. This helps to stabilize the colloidal dispersion and make the particle size distribution narrower.

Let us now discuss microgel formation as a function of HPC polymer concentration. In this experiment, the HPC concentration varied from 0.1 to 0.3 wt %, while the DTAB concentration and the reaction temperature were fixed at 1 cmc and 55 °C, respectively. Figure 3 shows hydrodynamic radius distributions ($f(R_h)$) of HPC microgel particles ($C = 8.94 \times 10^{-6}$ g/mL) in deionized water at 25 °C. The average radius $\langle R_h \rangle$ of the microgels becomes larger, and its distribution becomes broader with the increase of HPC concentration. This result may be explained in terms of interaction of surfactant DTAB with HPC. As the HPC concentration increases, the average number of absorbed surfactant aggregates on each HPC polymer chain should decrease, reducing the interaggregate electrostatic repulsion force. This causes HPC linear chains to become more aggregated at higher HPC concentration. Thus, the average radius $\langle R_h \rangle$ of the nanoparticles increases, and its distribution becomes broader.

The reaction temperature plays an important role for the formation of the HPC microgel particles. Figure 4 shows hydrodynamic radius distributions ($f(R_h)$) of HPC microgel particles ($C = 8.94 \times 10^{-6}$ g/mL) in deionized water at 25 °C. These particles were made at various reaction temperatures in 0.1 wt % HPC solution and at 1 cmc DTAB concentration. The reaction temperature at which microgels formed is in a small range within about 3 deg above the LCST, which is 55 °C for this dispersion. Below the LCST, we did not observe formation of HPC nanoparticles. In this range studied, as the reaction temperature increases, the average radius of the resultant microgels becomes larger and the radius distribution becomes broader.

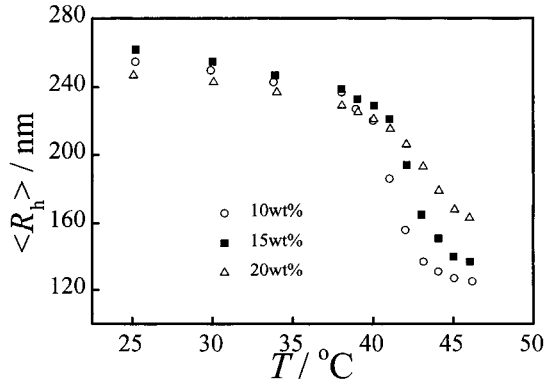

Figure 5. Average hydrodynamic radius $\langle R_h \rangle$ of HPC microgel with different cross-linking density changes as a function of temperature in deionized water. The microgels with 10 wt % cross-linking density were prepared in 0.5 wt % HPC solution at 1.5 cmc DTAB and at the reaction temperature 65 °C. This same batch of microgels was also used in Figures 6−8.

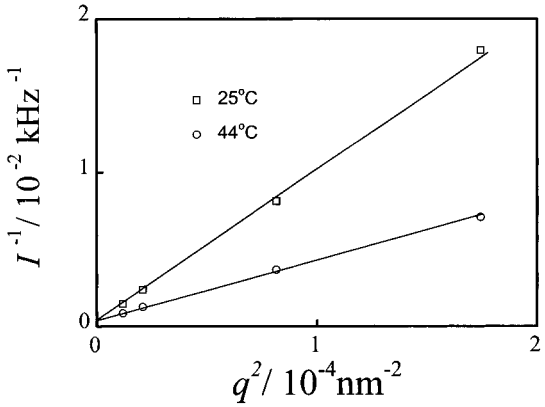

Figure 6. Inverse of time-averaged scattered intensity I^{-1} vs wave vector square q^2 of HPC microgel particles in deionized water at 25 and at 44 °C. The solid lines are the least-squares fit to the data.

The reaction temperature-dependent size of the microgels is related to the HPC hydrophobicity and the interaction of surfactant with the HPC. As the reaction temperature just reached LCST, the aggregated HPC chains can form stable nanoparticles due to intermicelle electrostatic repulsion. With the increase of reaction temperature above the LCST, the driving force of polymer−polymer aggregation increases. On the other hand, the interparticle electrostatic repulsion increases as particle size increases. As a result, more HPC chains aggregate to form larger particles until the new equilibrium between the hydrophobic interaction and intermicelle electrostatic repulsion is reached.

B. Characterization of HPC Microgels. The swelling properties of HPC microgels were characterized using light scattering techniques after exhaustive dialysis to wash out surfactant and residue chemicals. The HPC microgels undergo a volume phase transition in water from a swollen state to a collapsed state as the temperature increases. The driving forces for the thermal-sensitive volume phase transition were considered to be a balance between the hydrophilic and hydrophobic interactions of inter- and intrapolymer chains.

We first discuss the volume phase transition of HPC microgels at various cross-linker concentrations. The volume phase transition temperature, T_c, is defined as the one that causes the sharpest rate of the change in gel volume. The average hydrodynamic radius is plotted as a function of temperature as shown in Figure 5. Although up to 20 wt % of cross-linker relative to the HPC is used during synthesis, solubility properties of the linear HPC polymer are expected to dominate the gel swelling behavior. The average molar mass of the segment between two neighbored cross-linking points, $\bar{M}_c$, is inversely proportional to the cross-linking concentration. As a result, the degree of swelling at room temperature and the size change below and above T_c decrease with the increase of the cross-linking concentration. It is noted that the effective cross-linker concentration that actually contributes to the formation of the network is expected to be smaller than the one that was used in the polymerization process. This may be the main reason that the size contraction (about a factor 2 in Figure 5) is quite large when one considers the fairly high degrees of cross-linkers.

We then discuss the size distribution of microgels below and above T_c. The plot of inverse of the time-averaged scattered intensity I^{-1} versus the square of wavevector, q^2, is shown in Figure 6 for the microgel dispersion of concentration 8.94×10^{-6} g/mL in water and the weight ratio of polymer to cross-linker of 10 wt %. The extrapolation of q^2 to $q \rightarrow 0$ led to the same intercept at $\theta = 0$. This indicates that the microgels are still stable at 44 °C, which is above T_c. It is noted that the HPC microgels have no electric charge in its surface, in contrast to the NIPA microgels. Although the NIPA polymer does not have charges, the NIPA microgel particles have charges, which are sulfate and carboxyl groups that originate from the ionic free radical polymerization initiator.[1] Thus, stabilization of the HPC microgels at $T > T_c$ is different from that of the NIPA microgels. The stability of the HPC microgel particles could be due to the steric interactions between these particles. The steric interaction produces the energy barrier to prevent microgels from aggregation at the temperatures higher than T_c.[27]

Figure 7 shows intensity autocorrelation functions and corresponding hydrodynamic radius distributions ($f(R_h)$) of the HPC microgels of concentration of 8.94×10^{-6} g/mL in deionized water at 25 and 44 °C, respectively. At 25 °C, the size distribution is very broad. This may be attributed to the relative broad length distribution of the tangling HPC chains on the particle surface. Since the cross-linking was directly performed on the long polymer chains that have an average molecular weight of about 1 000 000, the variation of the length of the surface tangling chains could be quite large. As the microgels were heated above T_c, the loose surface tangling chains collapse, resulting in a narrower particle size distribution.

The salt effect on the phase transition temperature of a dilute HPC microgel dispersion was also investigated. Figure 8 shows the average hydrodynamic radius $\langle R_h \rangle$ as a function of temperature for HPC microgel particles ($C = 8.94 \times 10^{-6}$ g/mL) in water and in 0.9 wt % NaCl solution (0.15 mol L^{-1}, physiological ionic strength). T_c is about 41 °C for the microgels in pure water, while it is about 39 °C for the microgel in 0.9 wt % NaCl. The decrease of T_c with addition of NaCl may be because inorganic ions form hydrates through ion−dipole interactions.[28] The disturbance of water structure by adding NaCl in HPC dispersion induces contact between HPC polymer chains, causing the decrease of T_c of HPC microgels. Combining the temperature-responsive volume change, the suitable transition temperature around 39 °C under the physiological condition that corresponds to the temperature as a person gets a

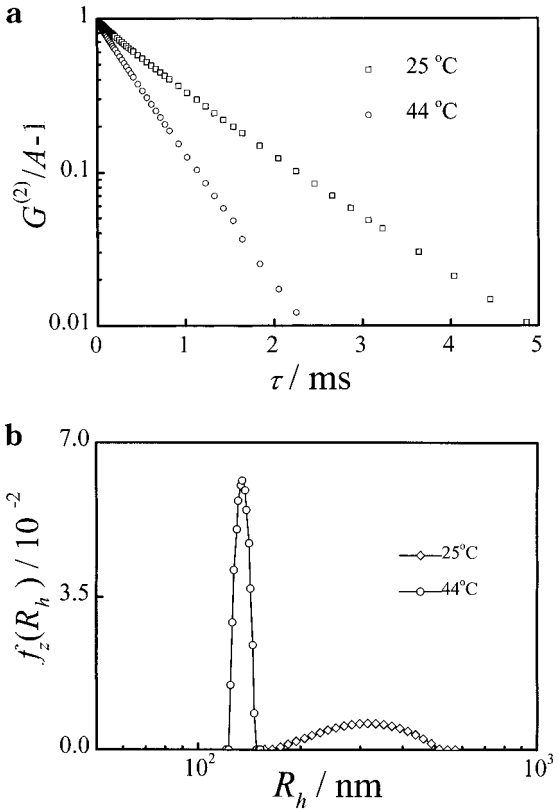

Figure 7. (a) Intensity autocorrelation functions of the HPC microgel in deionized water at 25 and 44 °C. (b) Corresponding hydrodynamic radius distributions ($f(R_h)$) of the samples.

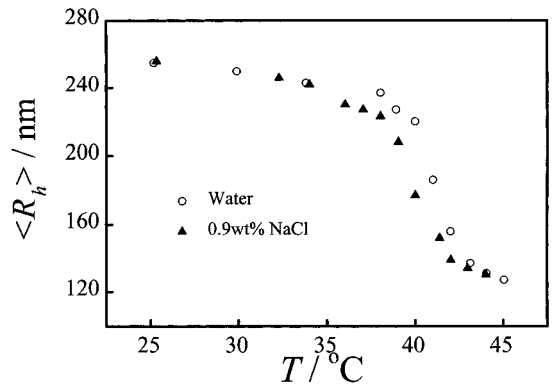

Figure 8. Average hydrodynamic radius $\langle R_h \rangle$ of HPC microgels changes as a function of temperature in deionized water and in 0.9 wt % NaCl aqueous solution.

fever, biocompatibility of the HPC, and uniformed and small size, the HPC microgels could be particularly useful in controlled drug delivery applications.

Conclusion

HPC microgels have been synthesized for the first time by chemically cross-linking hydroxypropyl cellulose (HPC) linear macromolecules. The controllable synthesis parameters—surfactant concentration, HPC concentration, and reaction temperature—were varied to determine the effects on the size and size distribution of the microgels as monitored using laser light scattering techniques. It is found that the microgels can form only above the cmc of the DTAB surfactant at the LCST. As the HPC concentration increases from 0.1 to 0.3 wt %, the size distribution becomes significantly broader. Furthermore, the reaction temperature plays an important role for the size distribution: upon the increase of the temperature above the LCST, the particle size increases quickly. The formation of microgels may be explained by the balance between hydrophobic interaction between HPC polymer chains and intermicelle electrostatic repulsion. The swelling and phase transition properties of the resultant HPC microgels are analyzed using both static and dynamic light scattering techniques as a function of temperature at various cross-linker concentrations. It is found that the increase in the cross-linker density reduces the shrinkage extent and increases the transition temperature. The dilute HPC microgel particles with concentration of 8.94×10^{-6} g/mL form a stable colloidal dispersion at room temperature and at 44 °C ($> T_c$), probably due to steric effect. In the aqueous solution of physiological salt concentration, the phase transition of the HPC microgels occurs at about 39 °C, which corresponds to a fever temperature of the human body. Combining the temperature-responsive volume change, biocompatibility of the HPC, and uniform and small size, the HPC microgels could be particularly useful in controlled drug delivery applications.

Acknowledgment is made to the donors of the Petroleum Research Fund, administered by the American Chemical Society, and to the U.S. Army Research Office under Grant DAAG55-98-1-0175 for support of this research.

References and Notes

(1) Pelton, R. *Adv. Colloid Interface Sci.* **2000**, *85*, 1.
(2) Saunders, B. R.; Vincent, B. *Adv. Colloid Interface Sci.* **1999**, *80*, 1.
(3) Murry, M. J.; Snowden, M. J. *Adv. Colloid Interface Sci.* **1995**, *54*, 73.
(4) Senff, H.; Richtering, W. *J. Chem. Phys.* **1999**, *111*, 1705.
(5) Li, Y.; Tanaka, T. *J. Chem. Phys.* **1990**, *40*, 820.
(6) Bradna, P.; Quadrat, Q.; Snuparck, *J. Colloid Polym. Sci.* **1995**, *273*, 324.
(7) Sasa, N.; Yamaoks, T. *Adv. Mater.* **1994**, *6*, 417.
(8) Sahoo, S. K.; De, T. K.; Ghosh, P. K.; Maitra, A. *J. Colloid Interface Sci.* **1998**, *206*, 361.
(9) Kiser, P. F.; Wilson, G.; Needham, D. *Nature* **1998**, *394*, 459.
(10) Pelton, R. H.; Chibante, P. *Colloids Surf.* **1986**, *120*, 247.
(11) Neyret, S.; Vincent, B. *Polymer* **1997**, *38*, 6129.
(12) Antionietti, M.; Pakula, T.; Bremser, W. *Macromolecules* **1995**, *28*, 4227.
(13) Frank, M.; Burchard, W. *Makromol. Chem. Rapid Commun.* **1991**, *12*, 64.
(14) Hirotsu, S.; Hirokawa, Y.; Tanaka, T. *J. Chem. Phys.* **1987**, *87*, 1392.
(15) Kabra, B. G.; Gehrke, S. H.; Spontak, R. J. *Macromolecules* **1998**, *31*, 2166.
(16) Harsh, D. C.; Gehrke, S. H. *J. Controlled Release* **1991**, *17*, 175.
(17) Winnik, F. M.; Tamai, N.; Yonezawa, J.; Nishimura, Y.; Yamazaki, I. *J. Phys. Chem.* **1992**, *96*, 1967.
(18) Wu, C. *Polymer* **1998**, *39*, 4609.
(19) Zhou, S.; Chu, B. *J. Phys. Chem. B* **1998**, *102*, 1364.
(20) Anbergen, U.; Oppermann, W. *Polymer* **1990**, *31*, 1854.
(21) Chu, B. *Laser Light Scattering*, 2nd ed.; Academic Press: New York, 1991.
(22) Karlstrom, G.; Carlsson, A.; Lindman, B. *J. Phys. Chem.* **1990**, *94*, 5005.
(23) Ahlnas, T.; Karlstrom, G.; Lindman, B. *J. Phys. Chem.* **1987**, *91*, 4030.
(24) Karlstrom, G. *J. Phys. Chem.* **1985**, *89*, 4962.
(25) Hormnirun, P.; Sirivat, A.; Jamieson, A. M. *Polymer* **2000**, *41*, 2127.
(26) Drummond, C. J.; Albers, S.; Furlong, D. N. *Colloids Surf.* **1992**, *62*, 75.
(27) Lashkevich, O. V.; Dyagileva, A. B.; Chernoberezhskii, Y. M. *Colloid J.* **1997**, *59*, 467.
(28) Inomata, H.; Goto, S.; Otake, K.; Saito, S. *Langmuir* **1992**, *8*, 687.

MA000776K